

# Epigenetically modulated miR-1224 suppresses the proliferation of HCC through CREB-mediated activation of YAP signaling pathway

Shikun Yang,<sup>1,3</sup> Wei Jiang,<sup>1,2,3</sup> Wenjie Yang,<sup>1,3</sup> Chao Yang,<sup>1,3</sup> Xinchun Yang,<sup>1</sup> Keyan Chen,<sup>1</sup> Yuanchang Hu,<sup>1</sup> Gefenqiang Shen,<sup>1</sup> Ling Lu,<sup>1</sup> Feng Cheng,<sup>1</sup> Feng Zhang,<sup>1</sup> Jianhua Rao,<sup>1</sup> and Xuehao Wang<sup>1</sup>

<sup>1</sup>Hepatobiliary/Liver Transplantation Center, The First Affiliated Hospital of Nanjing Medical University, Key Laboratory of Liver Transplantation, Chinese Academy of Medical Sciences, Nanjing 210029, China; <sup>2</sup>Department of Thoracic Surgery, The First Affiliated Hospital of Soochow University, Suzhou 210500, China

**Mounting evidence has demonstrated that microRNA-1224 (miR-1224) is commonly downregulated and serves as a tumor suppressor in multiple malignancies. However, the role and mechanisms responsible for miR-1224 in hepatocellular carcinoma (HCC) remain unclear. In this study, we found that the expression of miR-1224 was downregulated in HCC. Low miR-1224 expression was associated with poor clinicopathologic features and short overall survival. Moreover, the methylation status of putative CpG islands was also found to be an important part in the modulation of miR-1224 expression. miR-1224 could induce HCC cells to arrest in G0/G1 phase and inhibited the proliferation of HCC cells both *in vitro* and *in vivo*. Mechanistic investigation showed that by binding with cyclic AMP (cAMP)-response element binding protein (CREB) miR-1224 could repress the transcription and the activation of Yes-associated protein (YAP) signaling pathway. Furthermore, the expression of miR-1224 was inhibited by CREB through EZH2-mediated histone 3 lysine 27 (H3K27me3) on miR-1224 promoter, thus forming a positive feedback circuit. Our findings identify a miR-1224/CREB feedback loop for HCC progression and that blocking this circuit may represent a promising target for HCC treatment.**

## INTRODUCTION

Hepatocellular carcinoma (HCC) is the fifth most common malignant cancer and the second most frequent cause of cancer-related death worldwide, with approximately 81,080 new cases occurring every year.<sup>1</sup> Although therapeutic strategies, such as curative resection, liver transplantation, transarterial chemoembolization (TACE), and radiofrequency ablation have been applied previously, the long-term survival of HCC patients remains unsatisfactory.<sup>2,3</sup> In this regard, a more comprehensive understanding of the biological processes and mechanisms underlying HCC would contribute to the identification of novel preventative, diagnostic, and therapeutic targets, including non-coding RNAs.

MicroRNAs (miRNAs), a class of evolutionarily conserved small non-coding RNAs composed of 20–24 nucleotides, function as post-transcriptional suppressors by targeting 3' untranslated regions (3' UTRs)

of protein-coding genes.<sup>4</sup> Accumulating evidence has indicated that the dysregulation of miRNAs has been observed in a variety of disorders, particularly cancers.<sup>5</sup> Through targeting protein-coding gene transcripts, miRNAs are involved in almost all biological processes in cancer cells, including proliferation, apoptosis, metabolism, differentiation, migration, and tumorigenesis.<sup>6–8</sup> Recent studies have also demonstrated that the dysregulation of miRNAs plays a pivotal role in the development of HCC.<sup>9,10</sup>

miRNA-1224 is a newly identified miRNA, lying within one of the introns of the EIF2B5 gene located on human chromosome 3q27.1. Current evidence demonstrates that miR-1224 is commonly downregulated in a variety of malignancies including gastric cancer, lung cancer, and colorectal cancer and functions as a tumor suppressor via inhibiting migration, invasion, and cell proliferation or by promoting apoptosis and chemoresistance.<sup>11–13</sup> However, the expression and specific biological function and underlying mechanisms of miR-1224 have not been investigated in HCC.

In this study, we identified downregulation of miR-1224 in HCC tissues and cell lines. Furthermore, we revealed the inhibitory role of miR-1224 in the proliferation and tumorigenesis of HCC. Mechanistically, miR-1224 suppressed the proliferation of HCC cells by directly targeting CREB, which in turn inhibited miR-1224 levels through promoter histone methylation. Our results reveal a novel positive feedback loop between miR-1224 and CREB as a determinant of HCC proliferation and that blocking the feedback loop may effectively halt the progression of HCC.

Received 13 March 2020; accepted 8 January 2021;  
<https://doi.org/10.1016/j.omtn.2021.01.008>.

<sup>3</sup>These authors contributed equally

**Correspondence:** Xuehao Wang, Hepatobiliary and Liver Transplantation Center, The First Affiliated Hospital of Nanjing Medical University, Key Laboratory of Liver Transplantation, Chinese Academy of Medical Sciences, Nanjing 210029, China.  
**E-mail:** wangxh@njmu.edu.cn

**Correspondence:** Jianhua Rao, Hepatobiliary and Liver Transplantation Center, The First Affiliated Hospital of Nanjing Medical University, Key Laboratory of Liver Transplantation, Chinese Academy of Medical Sciences, Nanjing 210029, China.  
**E-mail:** raojh@njmu.edu.cn



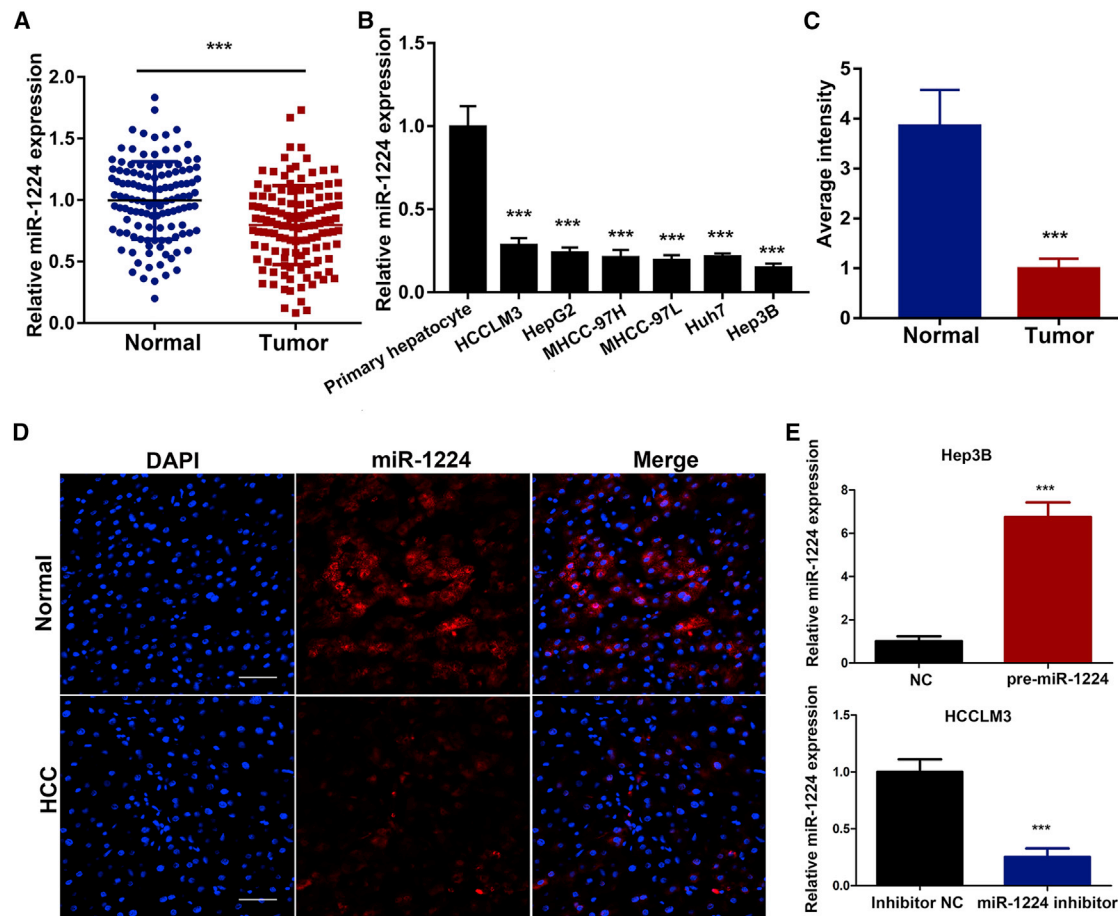


**Figure 1. miR-1224 is downregulated in HCC tissues and cell lines**

(A) miR-1224 expression in 124-paired human HCC and adjacent normal tissues by qPCR. (B) miR-1224 expression in HCC cell lines and human hepatocytes cells. (C and D) The expression of miR-1224 in HCC specimens and adjacent normal tissues as detected by FISH (scale bars, 50 μm). (E) Relative miR-1224 levels in Hep3B and HCCLM3 cells transfected with specific pre-miR-1224 or miR-1224 inhibitor, respectively. Cells transfected with empty lentiviral vectors served as a negative control (NC). \* $p < 0.05$ , \*\* $p < 0.01$ , \*\*\* $p < 0.001$ .

## RESULTS

### miR-1224 is downregulated in HCC tissues and cell lines

To investigate the clinicopathological significance of miR-1224 in HCC, we first determined the expression of miR-1224 in 124 pairs of HCC tissues and matched adjacent normal tissues by quantitative real-time PCR. Compared to adjacent samples, miR-1224 expression was significantly downregulated in HCC tissues (Figure 1A); these results were consistent with those arising from our fluorescence *in situ* hybridization (FISH) analysis (Figures 1C and 1D). Then, all patients were divided into a high miR-1224 expression group and a low miR-1224 expression group using the median level of miR-1224 as the cutoff value. As indicated in Table 1, low levels of miR-1224 were significantly correlated with tumor size ( $p = 0.007$ ), tumor node metastasis classification TNM stage (0.030), and advanced Edmondson grade ( $p = 0.017$ ). Additionally, patients with low expression of miR-1224 had poorer overall survival (OS) and disease-free survival (DFS; Figures S1A and S1B). Compared with the miR-1224 levels in normal liver cell lines, miR-

1224 levels were significantly lower in HCC cell lines, including HepG2, Hep3B, HCCLM3, MHCC97H, MHCC97-L, and Huh7 (Figure 1B) cells. Notably, Hep3B and HCCLM3 possessed relatively much lower and higher miR-1224 levels. Thus, we used Hep3B and HCCLM3 cells as models with which to investigate the effect of miR-1224 on HCC progression. We restored miR-1224 expression in the Hep3B cell line and inhibited its expression in the HCCLM3 cell line by lentivirus infection. The efficiency of overexpression or knockdown was validated by quantitative real-time PCR (Figure 1E). Taken together, our results suggested that the expression of miR-1224 was downregulated in HCC tissues and cell lines, and its downregulation was significantly associated with poor clinicopathological features.

### The methylation status of CpG islands epigenetic is involved in the regulation of miR-1224 expression

Accumulating evidence indicates that epigenetic mechanisms such as the methylation status of CpG islands might control the

**Table 1. Association between miR-1224 expression and clinicopathologic features of patients with hepatocellular carcinoma**

Variables	miR-1224 expression		p value
	High n = 62	Low n = 62	
<b>Age (years)</b>			
≤60	29	28	0.857
>60	33	34	
<b>Gender</b>			
Female	21	26	0.355
Male	41	36	
<b>HBs antigen</b>			
Absent	23	25	0.712
Present	39	37	
<b>Liver cirrhosis</b>			
With	43	39	0.448
Without	19	23	
<b>AFP (ng/mL)</b>			
≤200	29	20	0.098
>200	33	42	
<b>Tumor size</b>			
≤3 cm	39	24	0.007*
>3 cm	23	38	
<b>TNM stage</b>			
I–II	40	28	0.030*
III–IV	22	34	
<b>Edmondson grade</b>			
I–II	43	30	0.017*
III–IV	19	32	

\*p &lt; 0.05

expression of various miRNAs in cancers.<sup>14,15</sup> In our study, we predicted the transcript start site (TSS) of miR-1224 first. The explicit CpG island located near the miR-1224 TSS was identified by online software (<http://www.urogene.org/>; Figures 2A and 2B). Then, we further treated Hep3B and HCCLM3 cells with 5-aza-2'-deoxycytidine (5-aza-dc), an inhibitor of DNA methyltransferase, to identify the underlying relationship between miR-1224 expression and the methylation status of CpG islands. Results indicated that the expression of miR-1224 was sharply elevated in both of the two cell types after treatment with 5-aza-dc (Figure 2C). Finally, we carried out a bisulfite-sequencing PCR (BSP) assay to estimate the original methylation status of the CpG islands in both cell types. Our analyses indicated that DNA methylation levels in this region of Hep3B and HCCLM3 cell lines were extremely high (Figures 2D and 2E). Collectively, these data indicate that the high methylation levels of CpG islands may contribute to the downregulated expression of miR-1224 in HCC.

### miR-1224 suppressed HCC cell proliferation *in vitro*

To further investigate the effect of miR-1224 on the malignant progression of HCC, we carried out Cell Counting Kit-8 (CCK-8) assays, which showed that miR-1224 overexpression could notably inhibit cell proliferation in Hep3B cells, whereas the knockdown of miR-1224 could enhance the growth of Hep3B and HCCLM3 cells. (Figures 3A and 3B). Concordant with these results, colony-formation assays showed that ectopic miR-1224 expression impaired cell growth. Conversely, silencing miR-1224 increased the colony-forming ability of Hep3B and HCCLM3 cells (Figures 3C and 3D). In addition, 5-ethynyl-2-deoxyuridine (EdU) assays revealed compromised cell growth in cells transfected with pre-miR-1224 lentivirus, while miR-1224 knockdown promoted cell proliferation (Figure 3E). Collectively, these results strongly indicated that miR-1224 functions as a suppressor in HCC cells.

### miR-1224 induced G0/G1-phase arrest in HCC cells and inhibited the activation of YAP signaling pathway

Because miR-1224 markedly attenuated the ability of HCC cells to proliferate, we next aimed to define whether miR-1224 regulated the cell-cycle progression of HCC cells. Through analyzing cell-cycle distribution using fluorescence-activated cell sorting (FACS), we found that the overexpression of miR-1224 induced G0/G1-phase arrest in Hep3B cells and that knockdown of miR-1224 significantly reduced the percentage of HCCLM3 cells in G0/G1 phase with an obvious increase of cells in S phase (Figure 4A). At the same time, as the key molecules in cell-cycle regulation, the protein levels of proliferating cell nuclear antigen (PCNA), cyclin D1, and cyclin E1 were significantly reduced in HCC cells overexpressing miR-1224 while P27 was upregulated; this was consistent with the appearance of G0/G1-phase arrest (Figure 4B). In contrast, cells in which miR-1224 had been inhibited showed upregulated expression levels of PCNA, cyclin D1, and cyclin E1, coincident with a reduction in the levels of P27 (Figure 4B).

To further clarify the potential pathway regulated by miR-1224, we carried out a gene set enrichment analysis (GSEA) using miR-1224 expression as a phenotype from TCGA database and the result showed that miR-1224 expression was significantly associated with Hippo signaling pathway (Figure S1C). Thus, we examined the key molecule of Hippo pathway by western blot. However, neither overexpression nor knockdown of miR-1224 in HCC cells could change the protein levels of Mst1/2, Lats1/2, p-Lats1, and SAV1, but the total YAP protein (Figure 4B).

It has been reported that YAP, a crucial transcription factor, is a major negative-regulatory downstream effector of the Hippo pathway regulating cell proliferation.<sup>16,17</sup> In addition, YAP can upregulate the expression of cyclin proteins and downregulate the expression of p27.<sup>18,19</sup> Next, we determined whether YAP was involved in the miR-1224-induced inhibition of cell proliferation. Western blotting showed that miR-1224 could downregulate the levels of total YAP and nuclear YAP and that miR-1224 inhibition could increase the nuclear localization of YAP. These results indicated that the application

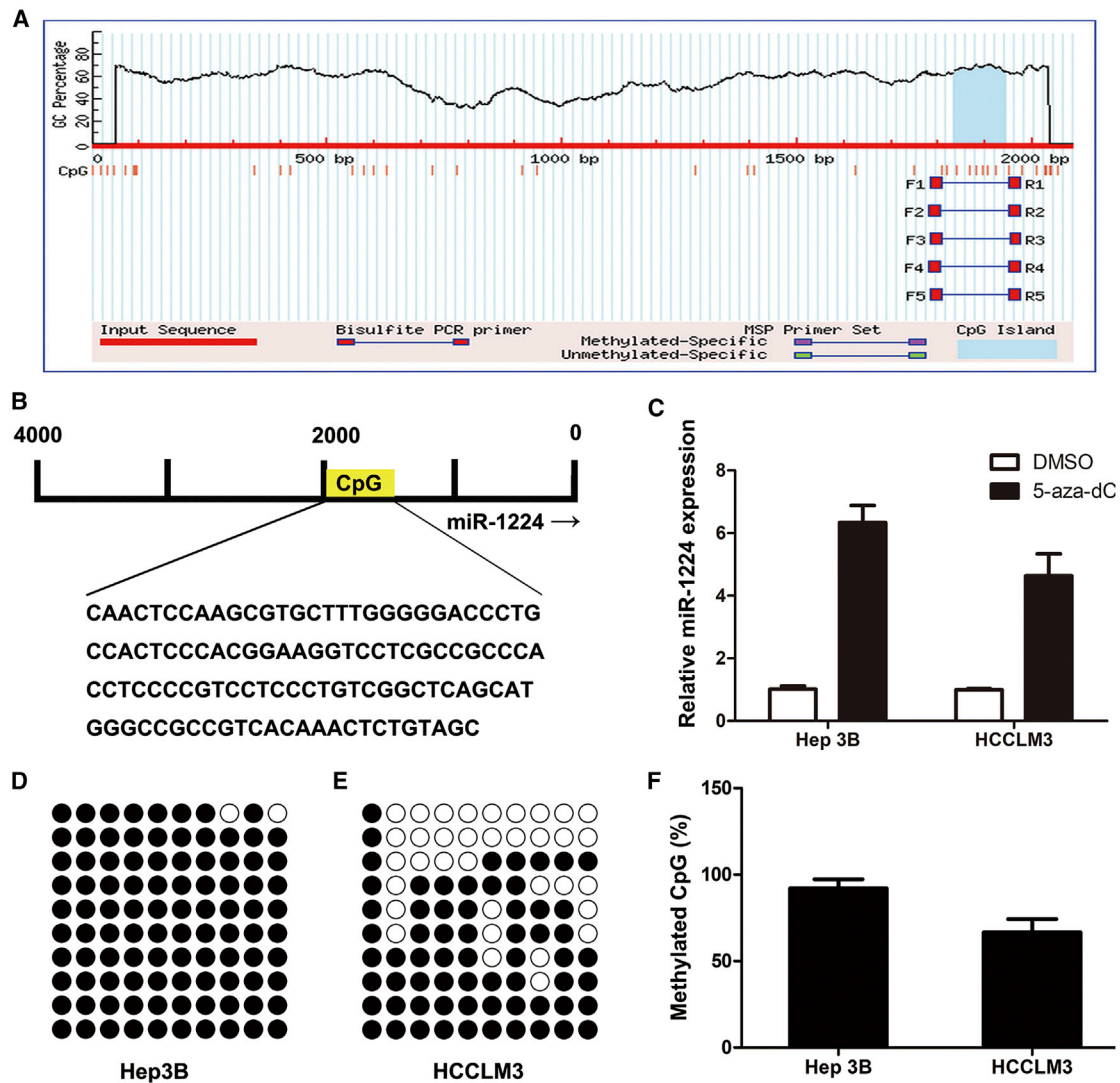


**Figure 2. The methylation status of CpG islands is involved in the regulation of miR-1224 expression**

(A and B) The DNA sequence of a CpG island in the miR-1224 promoter analyzed by BSP. (C and F) In contrast with DMSO, demethylation agent 5-aza-dC stimulated the expression of miR-1224 in HCC cell lines (Hep3B and HCCLM3). (D, E and F) Methylation profile of Hep3B and HCCLM3 cell lines. The open and filled circles symbolize the unmethylated and methylated CpGs, respectively. Ten colonies from each cell line were analyzed. Error bars represent the SD from ten randomly chosen colonies. \* $p < 0.05$ , \*\* $p < 0.01$ , \*\*\* $p < 0.001$ .

of a miR-1224 inhibitor could dramatically increase both the expression and the activity of YAP, while miR-1224 overexpression led to directly opposing effects (Figure 4B). As shown in Figure 4C, miR-1224 silencing enhanced nuclear retention of YAP in HCCLM3 cells, while miR-1224 overexpression reduced YAP nucleus retention in Hep3B cells. The hypothesis was further confirmed by quantitative real-time PCR, where overexpression of miR-1224 significantly decreased, while miR-1224 downregulation induced the transcription of YAP target genes, including CTGF and CYR61 (Figure 4D). According to this evidence, we suggest that miR-1224 might suppress HCC cell proliferation by activating Hippo signaling and that this occurs as a result of YAP nuclear localization.

#### miR-1224 directly targets CREB

Based on the molecular mechanism between miRNAs and mRNA, we attempted to ascertain the exact targets responsible for the observed effects of miR-1224 (described above). Using online bioinformatics databases (TargetScan, miRDB, and miRTarBase), we identified CREB and PPP1R9B as potential targets. All three databases predicted these two potential targets of miR-1224 (Figure 5A). We first tested the expression of PPP1R9B and found the PPP1R9B expression was upregulated more in HCC tissues than adjacent normal tissues (Figure S2A). However, the correlation analysis between miR-1224 and PPP1R9B mRNA was not statistically significant (Figure S2B). Moreover, neither the overexpression of miR-1224 nor miR-1224

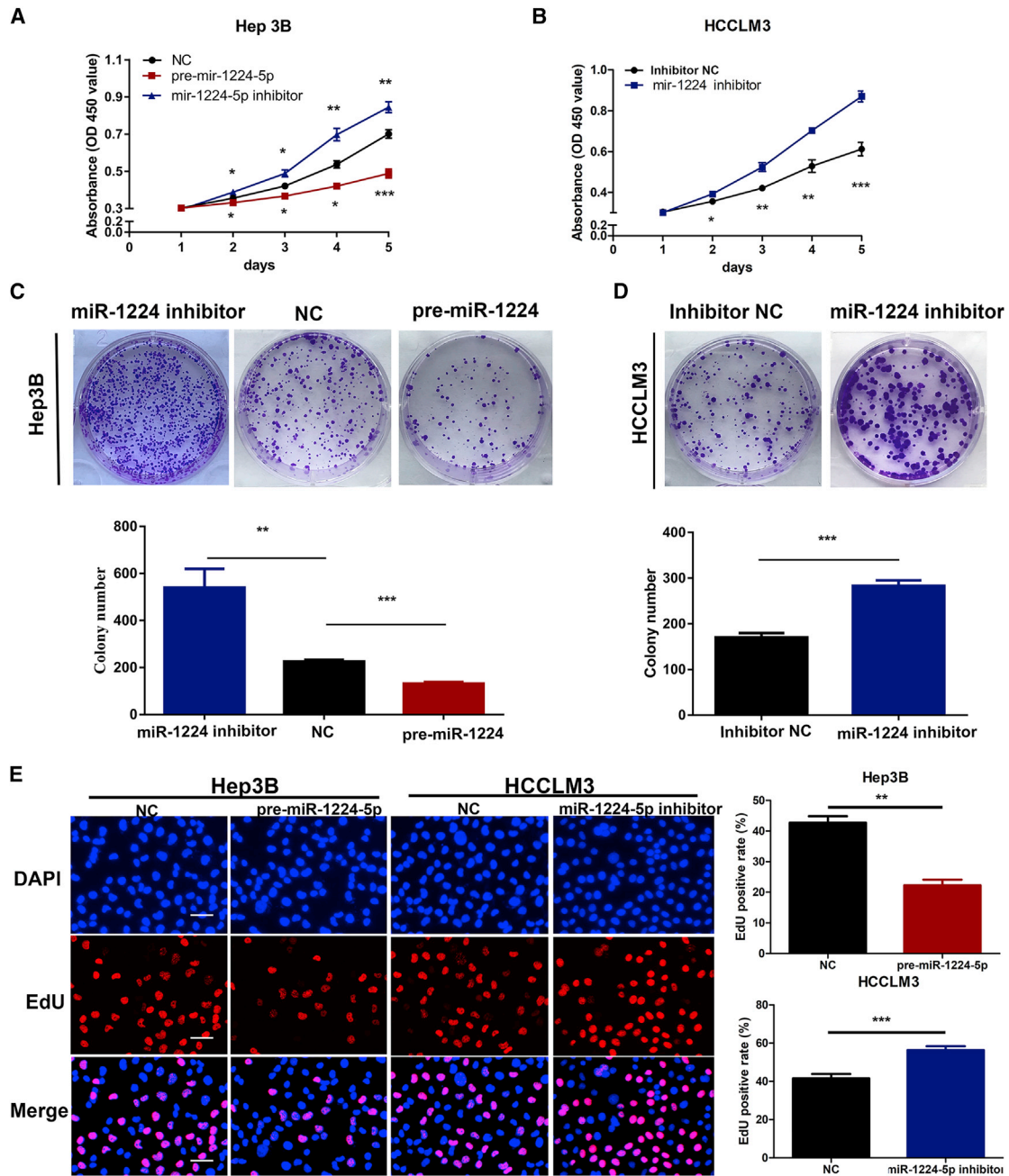
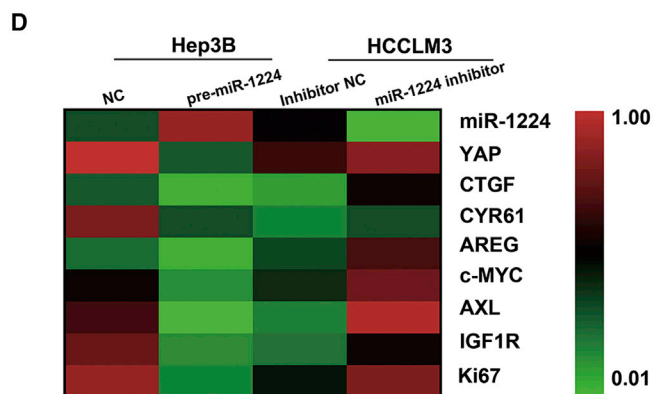
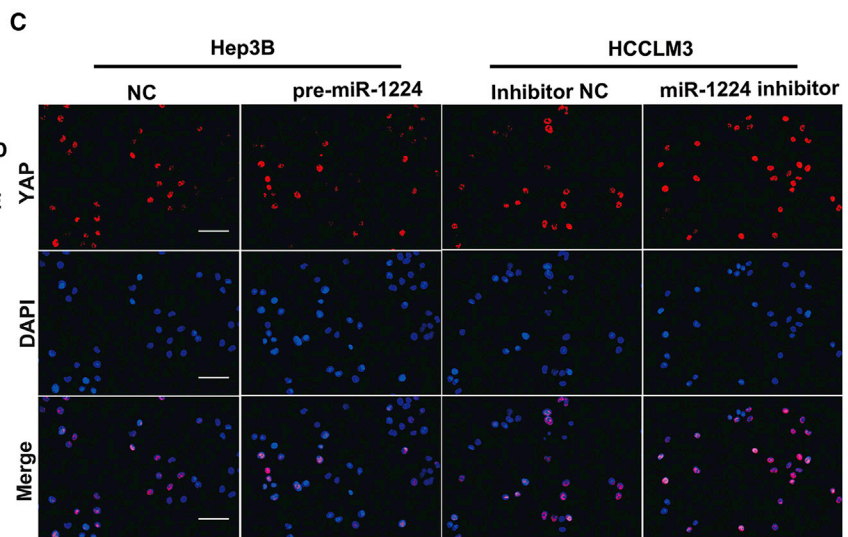
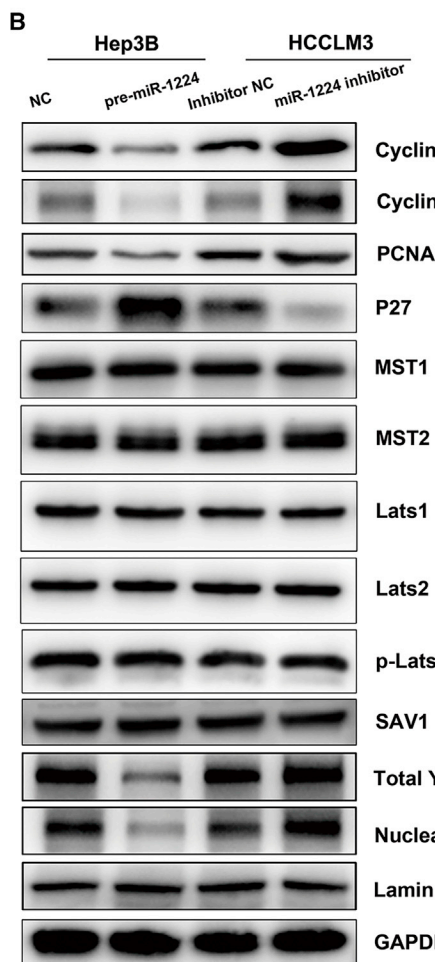
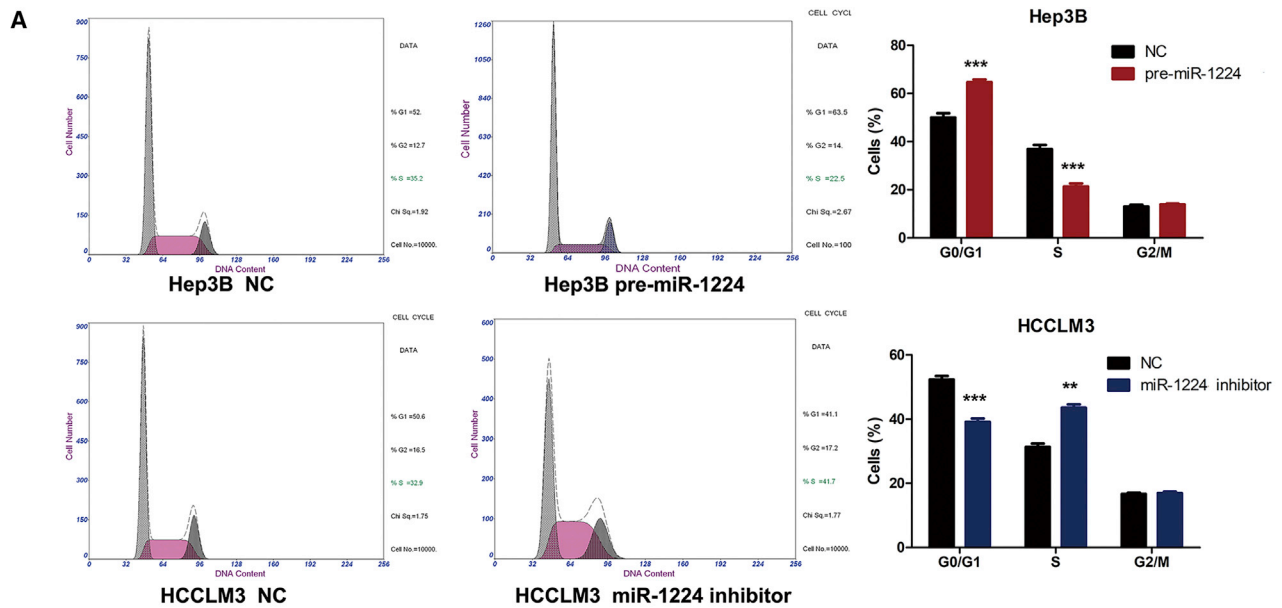


**Figure 3. miR-1224 suppressed HCC cell proliferation *in vitro***

(A and B) CCK-8 assays in Hep3B (A) and HCCLM3 (B) cells overexpressing or silencing miR-1224. Three duplicates were performed for each group, and three independent experiments were performed. (C and D) Colony-formation ability of miR-1224 overexpressing or silencing Hep3B and HCCLM3 cells. (E) 5-ethynyl-2'-deoxyuridine (EdU) incorporation assays were performed to assess cell proliferation in miR-1224 overexpressing or silencing Hep3B and HCCLM3 cells. EdU-positive cells were counted from three random microscopic fields for each well, and these experiments were repeated three times independently. All data are represented as means  $\pm$  SD. \* $p < 0.05$ , \*\* $p < 0.01$ , \*\*\* $p < 0.001$  compared with the NC. Scale bar, 50  $\mu\text{m}$ .

knockdown could alter the PPP1R9B levels (Figure S2C). Importantly, CREB plays a critical role in the regulation of YAP and acts as a regulator of proliferation in malignancies, including lung cancer

and pancreatic cancer, and the HCC was of particular interest.<sup>20–22</sup> Thus, we assumed that miR-1224 might exert its anti-tumor function by directly targeting CREB.



(legend on next page)

In the present study, we discovered that the expression level of CREB was widely upregulated in HCC tissues compared with adjacent normal tissues by qPCR and immunohistochemistry (IHC; Figures 5B and 5C). Quantitative real-time PCR was also used to examine the expression levels of CREB in HCC cell lines and primary human hepatocytes. These results further demonstrated that the level of CREB was markedly higher in HCC cell lines than human hepatocytes (Figure 5D). In addition, the overexpression of miR-1224 resulted in decreased levels of CREB protein, while miR-1224 knock-down led to the opposite results (Figure 5E). Moreover, an inverse correlation between miR-1224 and CREB mRNA was detected in HCC tissues (Figure 5F). To verify that the 3' UTR of CREB acted as a direct target for miR-1224, we conducted a luciferase reporter assay between miR-1224 and CREB to investigate direct interaction. Wild-type (WT) or mutated (MUT) 3' UTR target sites were cloned into a luciferase reporter vector. Ectopic miR-1224 expression could markedly inhibit the luciferase activity of the WT 3' UTR of CREB but not the MUT reporter, implying that miR-1224 targeted the 3' UTR of CREB and that point mutations in the site could abrogate this interaction (Figures 5G and 5H).

#### CREB overexpression partially reversed the effects of miR-1224 on HCC cell proliferation

To further illuminate that miR-1224 regulated HCC progression by targeting CREB, we transfected Hep3B pre-miR-1224 cells with CREB-plasmid to abolish the inhibition of CREB expression caused by miR-1224 and investigated CREB overexpression by quantitative real-time PCR and western blotting (Figures 6A and 6B). Importantly, the reintroduction of CREB significantly abolished the inhibitory effects of miR-1224 on cell proliferation, as verified by CCK-8 assays, EdU assays, and colony-formation assays (Figures 6C and 6D). Moreover, CREB overexpression reversed the G0/G1 cell-cycle arrest in Hep3B cells caused by miR-1224 (Figure 6E). Furthermore, overexpression of CREB could also activate YAP signaling by restoring the total and nuclear expression levels of YAP in HCC cells (Figure 6B). Taken together, our results support the fact that the miR-1224/CREB axis plays a critical role in regulating the proliferation process and distribution of the cell cycle in HCC cells.

#### miR-1224 suppressed HCC xenograft growth *in vivo*

To investigate whether miR-1224 could suppress the growth of tumor cells *in vivo*, we implanted Hep3B cells showing the stable overexpression of miR-1224, or HCCLM3 cells in which miR-1224 had been knocked down, into BALB/c nude mice. Mice were monitored every 3 days and euthanized in 5 weeks. Tumors derived from Hep3B pre-miR-1224 cells grew slower than those derived from Hep3B miR-

1224-negative control (NC) cells (Figures 7A and 7B). Compared with that in control mice, tumor weight in mice inoculated with Hep3B pre-miR-1224 cells was also distinctly lower at the fifth week (Figure 7C). In contrast, in mice inoculated with HCCLM3 miR-1224-inhibitor cells, mean tumor volume was obviously larger than that in the control group at the fifth week, and the tumors were also heavier (Figures 7A–7C).

Additionally, we investigated the expression level of miR-1224 in xenografts by quantitative real-time PCR. As shown in Figure 7D, increased miR-1224 expression was observed in the pre-miR-1224 group, while lower miR-1224 levels were observed in the miR-1224-inhibitor group. Xenografts were also analyzed by IHC to investigate the levels of CREB and YAP. Results showed that CREB expression levels were reduced in the pre-miR-1224 group, while elevated expression levels of CREB were detected in the miR-1224 inhibitor group (Figure 7E). Moreover, Ki-67 staining of xenograft tumors further confirmed the inhibitory effect of miR-1224 on HCC proliferation (Figure 7E). Overall, these results suggest that miR-1224 overexpression suppressed HCC proliferation *in vivo*, which are consistent with our *in vitro* results.

#### CREB inhibits miR-1224 transcription through EZH2-mediated promoter histone methylation

Accumulating evidence has indicated that regulatory feedback loops exist between miRNAs and target genes.<sup>23,24</sup> Interestingly, we found the levels of miR-1224 were markedly downregulated when CREB was overexpressed (Figure 8A). To determine how CREB regulates the expression of miR-1224, we detected the expression levels of pri-miR-1224 and pre-miR-1224 first. After upregulation of CREB, pri-miR-1224 levels and pre-miR-1224 levels were distinctly decreased (Figure 8B; Figure S3A), while knockdown of CREB (Figure S3B) could promote miR-1224 levels (Figure 8C; Figure S3C), which suggested that the transcription of miR-1224 was suppressed by CREB. Hence, we analyzed the putative promoter of EIF2B5 (miR-1224 is located in an intron of EIF2B5, and they have the same promoter), however, CREB had no direct interaction with the miR-1224 promoter, indicating that CREB did not inhibit the transcription of miR-1224 directly.

Epigenetic regulation, such as DNA methylation and histone modifications, play an important role in gene-expression regulation;<sup>25,26</sup> thus we hypothesized whether epigenetic alterations were involved in CREB-induced inhibition of miR-1224. Given our previous results that DNA methylation could downregulate the expression of miR-1224, we treated CREB-overexpressed HCC cells with 5-aza-dc. However, the results showed that 5-aza-dc could not reverse the effects of

#### Figure 4. miR-1224 induced G0/G1-phase arrest in HCC cells and inhibited the YAP signaling pathway

(A) Flow cytometry results showing the cell-cycle distribution of miR-1224 overexpressing or silencing Hep3B and HCCLM3 cells. (B) Representative western blotting bands showing the expression levels of PCNA, cyclin D1, cyclin E1, P27, and key regulators in the Hippo pathway in Hep3B and HCCLM3 cells with upregulated or downregulated miR-1224 expression. (C) Immunofluorescence analysis of nuclear retention and transcriptional activity of YAP in Hep3B and HCCLM3 cells transfected with pre-miR-1224 or miR-1224 inhibitor. Scale bar, 20  $\mu$ m. (D) Quantitative real-time PCR detection of YAP-target genes expression affected by miR-1224 in Hep3B and HCCLM3 cells. \* $p$  < 0.05, \*\* $p$  < 0.01 compared with the NC group. All data are represented as means  $\pm$  SD.

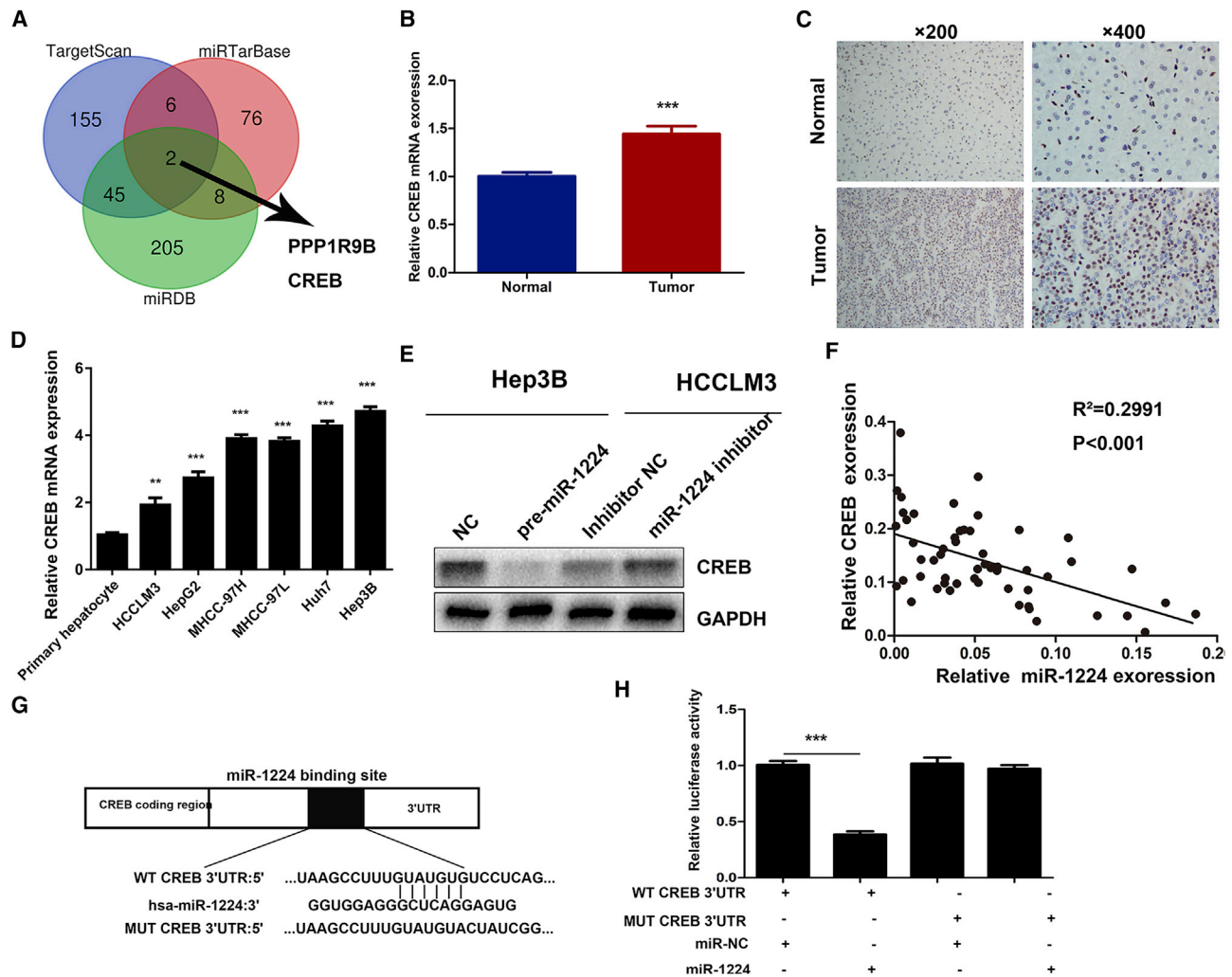


**Figure 5. miR-1224 directly targets CREB**

(A) Venn diagram showing that miR-1224 was predicted to target CREB by three different prediction algorithms: TargetScan, miRDB, and miRTarBase. (B) The expression levels of CREB mRNA in 60 pairs of HCC tissues and corresponding peritumor tissues were measured by quantitative real-time PCR. (C) Representative immunostaining images of HIF-1 $\alpha$  in HCC tissues and corresponding peritumor samples. Immunostaining images using secondary antibody alone are shown as controls. (D) CREB mRNA expression levels were examined in six HCC cell lines (Hep3B, HepG2, HCC97H, HCC97L, HCCLM3, and Huh7), and human hepatocytes. Three independent experiments were performed per group. (E) Western blotting analysis indicated that CREB expression levels were decreased in Hep3B cells with miR-1224 overexpression but increased in miR-1224-silenced HCCLM3 cells. GAPDH was used as the loading control. (F) Spearman correlation analysis was utilized to confirm the correlations between the HCCREB mRNA and miR-1224 expression levels in 60 HCC samples ( $r^2 = 0.2991$ ,  $p < 0.001$ ). (G) Predicted miR-1224 targeting sequence in CREB 3' UTR (WT CREB 3' UTR). Target sequences of CREB 3' UTR were mutated (MUT CREB 3' UTR). (H) Dual-luciferase reporter assay analysis of the effects of miR-1224 expression on the activities of WT and MUT CREB9 3'-UTR in 293 T cells. \* $p < 0.05$ , \*\* $p < 0.01$ , \*\*\* $p < 0.001$ . All data are represented as means  $\pm$  SD.

CREB on pri-miR-1224 level (Figure S3D), suggesting that DNA methylation was excluded in CREB-mediated miR-1224 downregulation.

Recently, CREB has been reported to enhance the epigenetic activity of enhancer of zeste homolog 2 (EZH2).<sup>27</sup> As the key component of polycomb-repressive complex 2 (PRC2), EZH2 catalyzed trimethylation on the histone 3 lysine 27 (H3K27me3), functioning as a transcription repressor. Consequently, we postulated that EZH2 was

involved in CREB-inhibited miR-1224 expression. Consistent with the earlier study, CREB promoted the activity of EZH2 in HCC cells, as assessed by H3K27me3 level (Figure 8D).

To further ascertain the role of EZH2 in CREB-elicited regulation of miR-1224 expression, we treated CREB-overexpressed HCCLM3 cells with EZH2 inhibitor GSK126, and the results showed that CREB could no longer induce the downregulation of pri-miR-1224 when HCCLM3 cells were co-treated with GSK126 (Figure 8E).

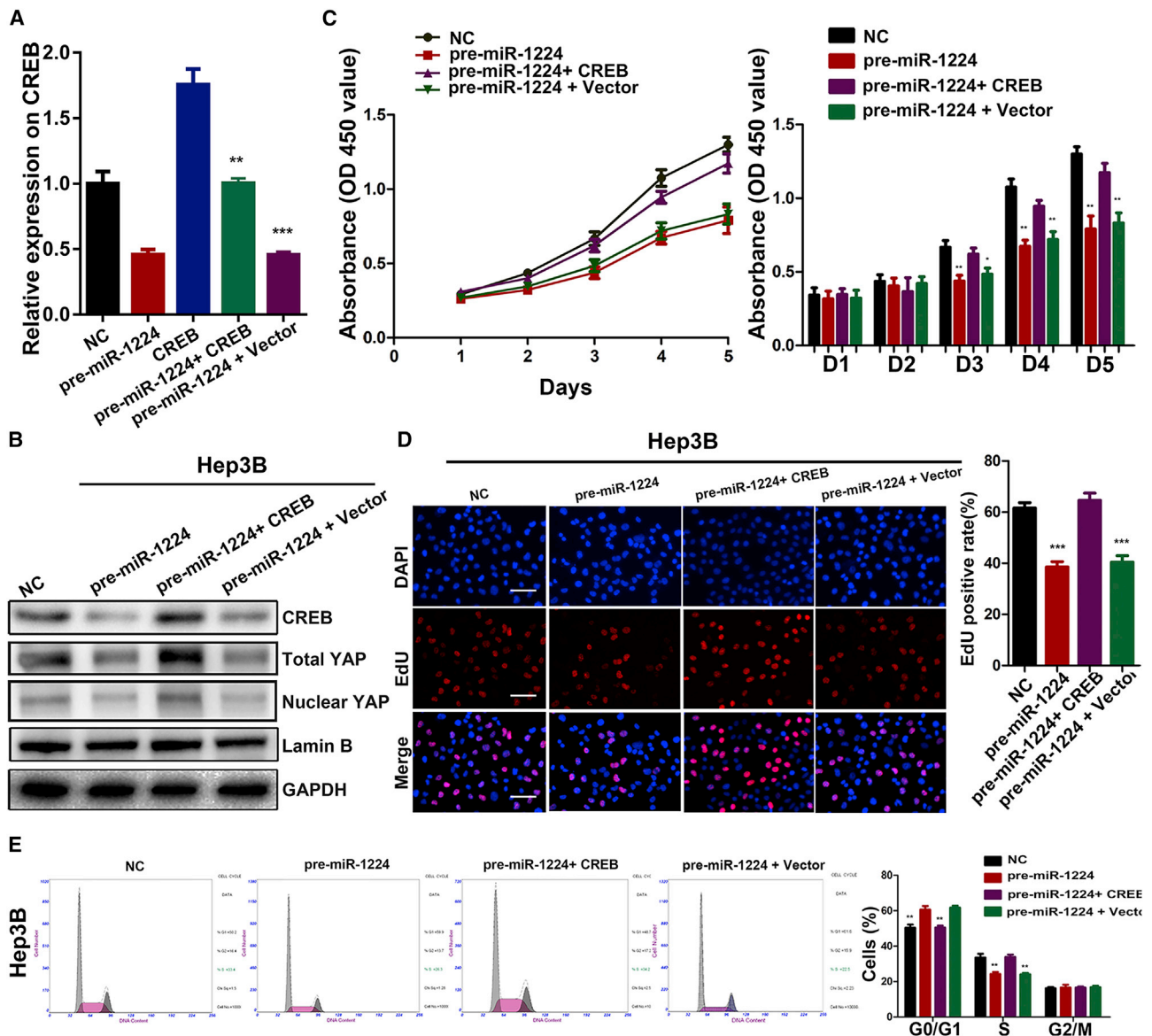


**Figure 6. CREB overexpression partially reversed the effects of miR-1224 on HCC cell proliferation**

(A) Expression of CREB mRNA in Hep3B cells transfected with miR-1224 overexpression lentivirus (pre-miR-1224) and CREB overexpression lentivirus (CREB). (B) Expression of CREB, total YAP and nuclear YAP, and GAPDH and lamin B at the protein level in Hep3B cells. (C) CCK-8 analysis of Hep3B-pre-miR-1224 cells transfected with CREB or vector. (D) EdU incorporation analysis of miR-1224-NC, pre-miR-1224, pre-miR-1224 plus CREB, and pre-miR-1224 plus vector in Hep-3B cells. EdU-positive cells were counted from three random microscopic fields for each well. Scale bar, 50  $\mu$ m. (E) Cell-cycle analysis of Hep-3B-pre-miR-1224 cells transfected with CREB or vector. \* $p < 0.05$ , \*\* $p < 0.01$ , \*\*\* $p < 0.001$ . All data are represented as means  $\pm$  SD.

Then, chromatin immunoprecipitation (ChIP) assay with H3K27me3 antibody and PCR targeting different regions of miR-1224 promoter were conducted (Figure S3E). We found much more H3K27me3 occupation at miR-1224 promoter region approximately  $-778$  to  $-585$  bp (as amplified by primer 4) in HCCLM3-CREB cells than control cells (Figure 8F; Figure S3E). However, GSK126 treatment overturned CREB-induced enrichment of H3K27me3 at the promoter of miR-1224 (Figure 8G). Collectively, these data suggested

that CREB-caused suppression of miR-1224 in HCC cells was dependent on EZH2-mediated H3K27me3 and transcription inhibition of pri-miR-1224, implicating a miR-1224 feedback loop in HCC progression.

## DISCUSSION

The tumorigenesis and progression of HCC is influenced by a range of events, through which HCC cells undergo a series of epigenetic and

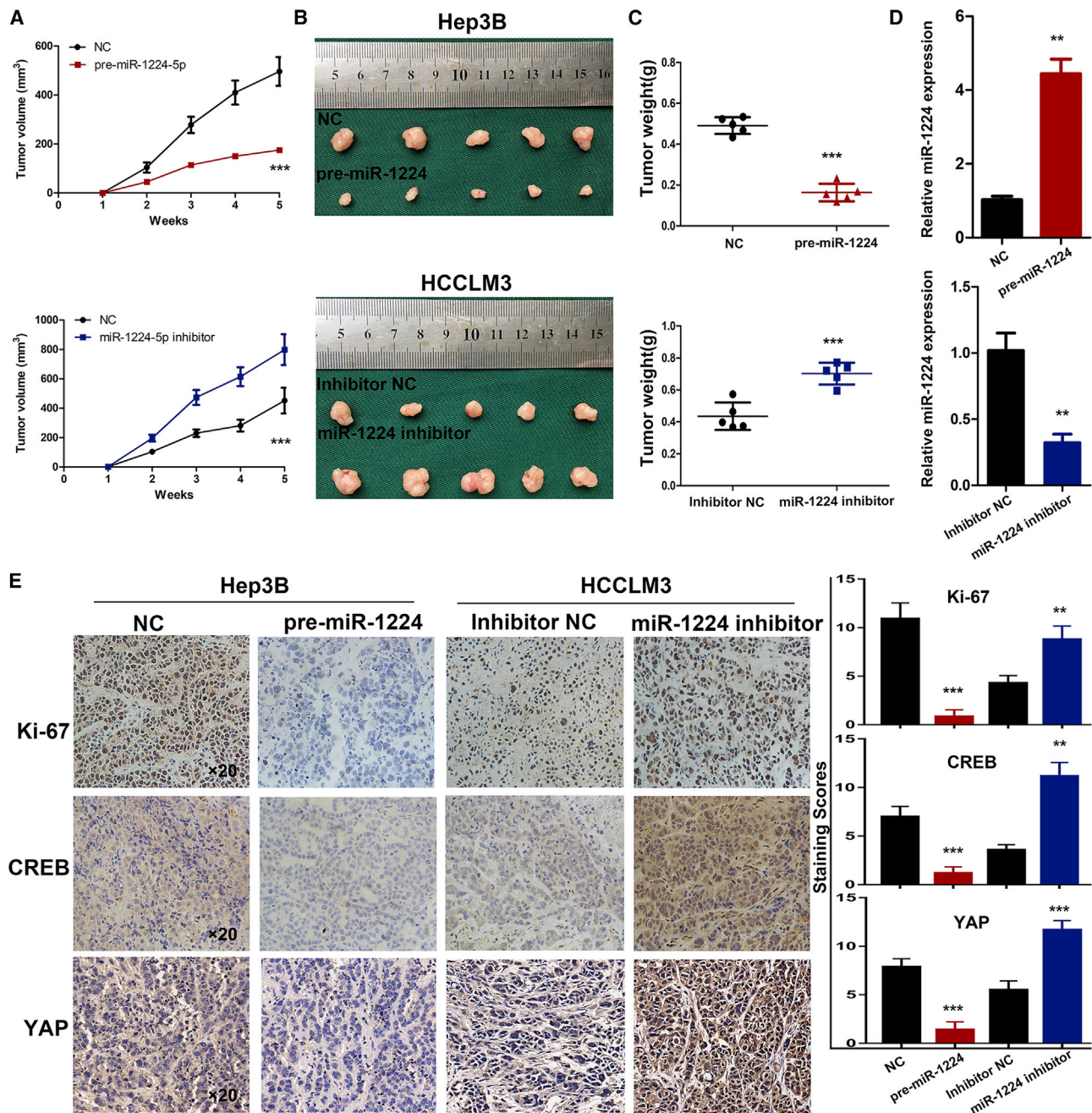


**Figure 7. miR-1224 suppressed HCC xenograft growth *in vivo***

(A–C) Tumor xenograft model. (A) growth curves for tumor volumes (n = 5 per group). Tumor volume was calculated based on the following equation: volume (mm<sup>3</sup>) = length (mm) × width<sup>2</sup>(mm<sup>2</sup>) × 0.5. (B) photographs of tumors. (C) Tumor weight of the xenografts derived from mice inoculated with Hep3B and HCCLM3 cells (n = 5 per group). (D) miR-1224 expression levels were analyzed by quantitative real-time PCR in Hep3B and HCCLM3 xenografts. (E) Representative immunostaining images showing Ki-67, CREB, and YAP levels in tumors derived from mice inoculated with Hep3B and HCCLM3 cells. Three independent experiments were performed for each group. \*p < 0.05, \*\*p < 0.01, \*\*\*p < 0.001. All data are presented as means ± SD.

genetic transformations in key growth regulatory genes that endow cancer cells with proliferative and survival advantages.<sup>28</sup> A number of studies have demonstrated the potency of miRNAs as significant

prognostic or diagnostic biomarkers and as promising therapeutics for malignant tumors. Furthermore, the dysregulation of miRNAs in HCC have been extensively profiled, but the precise function of

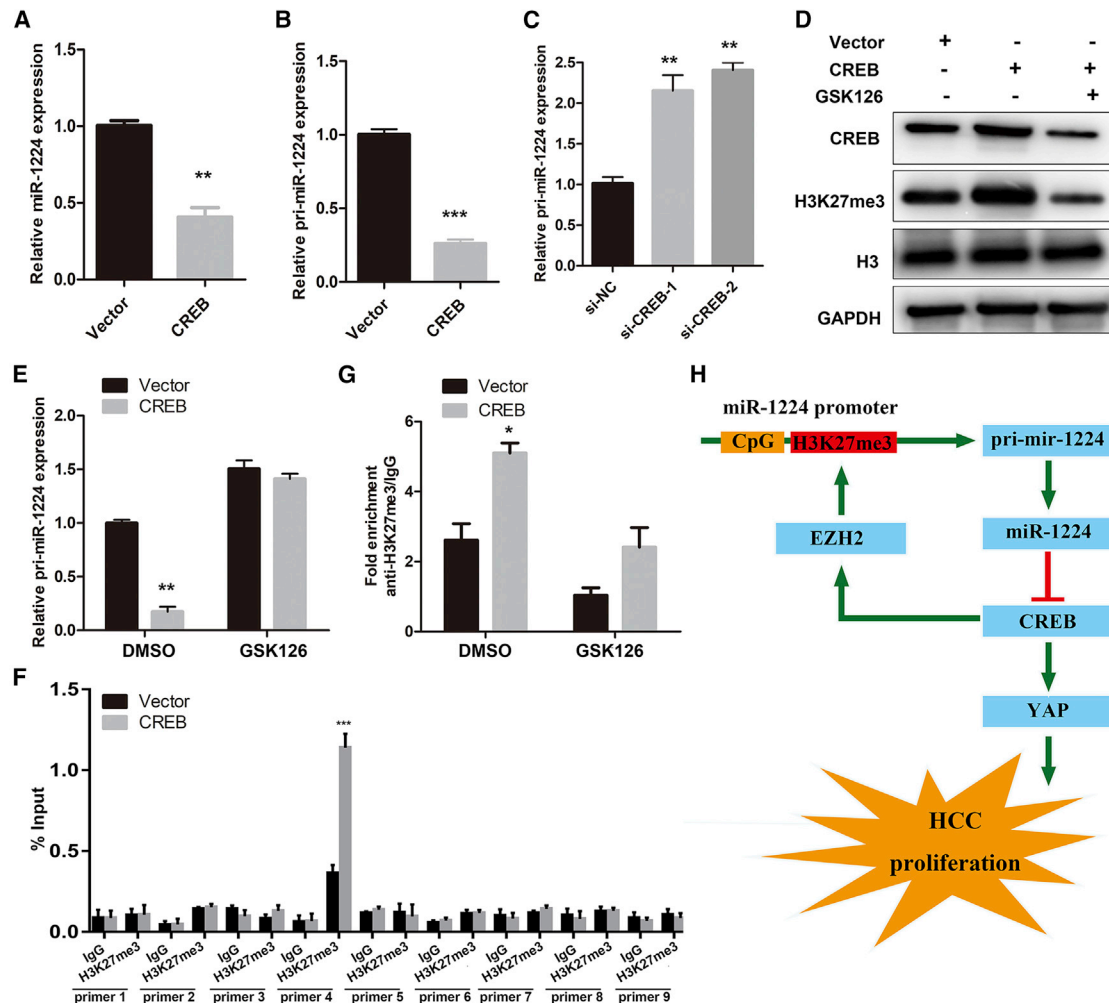


**Figure 8. CREB inhibits miR-1224 transcription through EZH2-mediated promoter histone methylation**

(A) Expression of miR-1224 in HCCLM3 cells transfected with control vector or CREB-expressing plasmid. (B) Expression of pri-miR-1224 in HCCLM3 cells transfected with control vector or CREB-expressing plasmid. (C) Expression of pri-miR-1224 in HCCLM3 cells with CREB knockdown. (D) Expression of CREB and H3K27me3 in CREB-overexpressed HCCLM3 cells treated with or without EZH2 inhibitors GSK126 (5  $\mu$ M) for 48 h. (E) Expression of pri-miR-1224 in HCCLM3 cells transfected with control vector or CREB-expressing plasmid after treatment of GSK126 (5  $\mu$ M) for 48 h. (F) ChIP-qPCR was performed to determine the interaction between H3K27me3 and miR-1224 promoter amplified by primer 4. (G) ChIP assay of the enrichment of H3K27me3 on miR-1224 promoter relative to IgG in indicated HCCLM3 cells. (H) Schematic representation of the mechanism of miR-1224/CREB circuit in the regulation of HCC proliferation. \* $p < 0.05$ , \*\* $p < 0.01$ , \*\*\* $p < 0.001$ . All data are presented as means  $\pm$  SD.

most dysregulated miRNAs in the proliferation and metastasis of HCC still remains unclear. Elucidating the association of these miRNAs with HCC progression may be of great importance in identifying novel therapeutic options and to improve the clinical prognosis.

Human miR-1224 is transcribed from chromosomal locus 3q27.1, which belongs to an intronic region of the EIF2B5 gene. It has been reported that miR-1224 is downregulated and functions as a pivotal tumor suppressor in multiple malignancies.<sup>12,29</sup> Although miR-1224 could inhibit proliferation in tumor endothelial cells of HCC,<sup>30</sup> the expression pattern of miR-1224, and its role in the tumorigenesis of HCC, have yet to be verified. In our study, we found that the basic expression levels of miR-1224 in HCC tissues and HCC cell

lines were drastically downregulated compared with adjacent normal liver tissues and a normal liver cell line, respectively. The specific mechanisms underlying the downregulation of miR-1224 in various human tumors remain unclear. We also find that the methylation status of CpG islands and histone modifications resulted in epigenetic regulation of miR-1224 expression in HCC cells.

Furthermore, we demonstrated that the low expression of miR-1224 was associated with unfavorable clinicopathological features of HCC. We revealed that miR-1224 could suppress the proliferation of HCC cells both *in vitro* and *in vivo* and that this effect was dependent on its role in the induction of cell-cycle events. The mechanism by which miR-1224 induced the suppression of cell proliferation

could be partially due to G0/G1-phase arrest caused by activation of the Hippo signaling pathway. Increasing evidence has established the inhibitory role of the Hippo pathway in tumorigenesis in a variety of cancers, especially those in the liver.<sup>17,31,32</sup> The Hippo pathway was first discovered in *Drosophila* and is a critical well-conserved regulator of organ size.<sup>33,34</sup> In mammals, activation of Hippo pathway results in stimulation of the serine/threonine kinases MST1/2, which subsequently phosphorylate the downstream kinases LATS1/2. YAP is the major downstream effector of the Hippo pathway; when YAP is phosphorylated by phosphorylated LATS1/2, this leads to cytoplasmic retention and proteolytic degradation.<sup>17,35</sup> Conversely, Hippo pathway inactivation contributes to dephosphorylation of YAP and prevents its export from the nucleus, thus promoting its transcriptional activities by interacting with a target gene such as Ki-67, *c-myc*, connective tissue growth factor (CTGF);<sup>36,37</sup> this results in tumor formation, cell proliferation, and the evasion of apoptosis and immune reaction.<sup>38–40</sup> Moreover, previous reports have indicated that CTGF could contribute to the upregulation of cyclin proteins and the downregulation of p27.<sup>18,19</sup> In the present study, we found that miR-1224 could decrease YAP expression and its nuclear localization and strongly reduce the transcriptional activity of YAP in HCC cells, thus revealing a novel mechanism in the regulation of HCC cell proliferation.

Based on the basic interactions between miRNA and mRNA, and the impact of miR-1224 upon the Hippo pathway, we further investigated the exact mechanism of miR-1224 in the regulating HCC cells proliferation. We identified CREB as a direct target, consistent with a previous study in malignant gliomas,<sup>41</sup> and upstream regulator of miR-1224, forming a feedback loop in HCC proliferation (Figure 8H). Accumulating evidence has established the proto-oncogenic role of CREB in tumorigenesis in many different types of malignancies.<sup>42,43</sup> For instance, previous studies have indicated that CREB was ubiquitously overexpressed in almost all malignant tumors and the overexpression of CREB could dramatically promote tumor proliferation and tumorigenesis such as lung, pancreatic, and liver cancer.<sup>21,44</sup> Moreover, the expression levels of CREB in HCC have been shown to be negatively correlated with patient prognosis.<sup>45</sup> Further *in vitro* experiments proved that the upregulation of CREB in HCC could promote the proliferation of cancer cells by enhancing the promoter activity of YAP;<sup>22,46</sup> this is consistent with the results of our present study. This evidence suggests that therapeutics targeting the miR-1224/CREB feedback loop might effectively halt the progression of HCC.

Mounting evidence has established that regulatory feedback circuits are substantial mechanisms of tumor biology. Based on our observations, the miR-1224/CREB feedback loop plays a critical role in the development of HCC. The feedback circuit may frame a broadly conserved module that boosts HCC cell proliferation. Some therapeutics or specific inhibitors that could reduce the activity of CREB or YAP might break the substantial mechanisms for tumor progression. Furthermore, great advances in miRNA-based bio-therapeutics have

made it of great promise as therapeutic approach.<sup>47–50</sup> In this case, it is essential to identify key miRNAs related to tumor progression. Given the important role of miR-1224 in HCC, delivery of miR-1224 to tumors may be a promising way for HCC treatment. For further clinical application, delivering miR-1224 through nanoparticles or cell-derived membrane vesicles carriers such as exosomes, could be more feasible. The effect of delivering miR-1224 in cancer treatment remains to be investigated, but it would certainly be of considerable significance in the future.

In summary, we found that the downregulation of miR-1224 in HCC was strongly correlated with poor clinicopathological features and prognosis. Our results revealed a novel positive feedback loop involving miR-1224 and CREB, in which miR-1224 suppressed tumor proliferation by suppressing the CREB/YAP axis and were inhibited by CREB/EZH2-mediated transcriptional suppression. Collectively, blocking the miR-1224/CREB circuit may therefore represent a promising therapeutic candidate for HCC.

## MATERIALS AND METHODS

### HCC samples and cell lines

Patient samples (n = 124) were randomly collected from consenting patients undergoing curative resection for HCC between 2012 and 2014 in The First Affiliated Hospital of Nanjing Medical University. All cases were diagnosed by three independent pathologists. HCC tissues and adjacent non-tumor tissues were collected immediately after resection and stored in liquid nitrogen for subsequent RNA and protein extraction.

Human primary hepatocytes were isolated from liver resections of patients undergoing partial hepatectomy, using a modified two-step collagenase perfusion technique, as previously described.<sup>51</sup>

The human HCC cell lines Hep3B, HCCLM3, HepG2, MHCC97-L, Huh7, and MHCC97-H were obtained from the Chinese Academy of Sciences Cell Bank (Shanghai, China) and cultured in Dulbecco's modified Eagle's medium (DMEM) (Invitrogen, Carlsbad, CA, USA) supplemented with 10% heat-inactivated fetal bovine serum (FBS), 100 U/mL of penicillin, and 100 mg/mL of streptomycin (Invitrogen). All cells were incubated in a humidified atmosphere with 5% CO<sub>2</sub> at 37°C.

### CCK-8 assay

Stable transfected HCCLM3 and Hep3B cells were seeded into 96-well plates at a density of  $1 \times 10^3$  cells per well and then cultured with 100  $\mu$ L of culture medium for 1, 2, 3, 4, and 5 days before adding 10  $\mu$ L of CCK-8 solution (Dojindo Laboratories, Kumamoto, Japan) to each well. After a 2 h incubation at 37°C, we measured the absorbance at 450 nm and used these data to calculate cell viability. Three independent experiments were performed.

### Colony-formation assay

Cells that had been transfected were harvested and then seeded in a 6-well plate (500 cells/well) and cultured for approximately 2 weeks

until colony formation was observed. Then, colonies were fixed with 4% paraformaldehyde and stained with 1% crystal violet. Colony-formation numbers were used to assess post-transfection cell proliferation. Three independent experiments were performed.

#### EdU assay

Cells ( $2 \times 10^5$ ) that had been transfected were incubated with EdU (RiboBio, Guangzhou, China) for 2 h at 37°C, fixed in 4% paraformaldehyde, permeabilized with 0.5% Triton-X, and stained with 1× Apollo reaction cocktail for 30 min and Hoechst 33342 according to the manufacturer's protocol. Subsequently, EdU-positive cells were visualized under a fluorescence microscope. Three independent experiments were repeated.

#### Cell-cycle assay

HCC cells were treated with trypsin after transfection and then collected by centrifugation for 5 min at 1,000 rpm. The collected cells were ruptured in 75% cold alcohol and stored at 4°C overnight. Subsequently, the fixed cells were washed with phosphate-buffered saline (PBS) and stained using a Cell Cycle Staining Kit (Multi-Sciences, Hangzhou, China) for 15 min before flow cytometry analysis.

#### Cell transfection

A lentiviral packaging kit was purchased from GenePharma (Shanghai, China). Three forms of lentivirus carrying hsa-miR-1224 (pre-miR-1224: 5'-GUGAGGACUCGGGAGGUG-3'), anti-miR-1224 (miR-1224-inhibitor: 5'-CCACCUCCCGAGUCCUCAC-3'), or a NC (miR-1224-NC: 5'-UUUGUACUACACAAAAGUACUG-3' and miR-1224-NC: 5'-CAGUACUUUGUGUAGUACAAA-3') were infected into the HCC cell line, Hep3B and HCCLM3 cells, according to the manufacturer's protocol.

This was followed by puromycin (7 µg/mL, Sigma-Aldrich) selection for a week, ultimately establishing stable cell lines. Overexpression plasmid vector and small interfering RNA (siRNA) for CREB were synthesized by Genomeditech Gene (Shanghai, China). Using Lipofectamine 3000 (Invitrogen), HCC cells were transfected according to the manufacturer's instructions.

#### RNA isolation and quantitative real-time PCR

Total RNA was isolated from human tissues or harvested cells with Trizol reagent (Invitrogen). Reverse transcription was then performed using the PrimeScript RT reagent Kit (Takara, Dalian, China). The expression levels of miR-1224 were then measured using the stem-loop-specific primer method. Bulge-loop miRNA quantitative real-time PCR Primer Sets (one RT primer and a pair of qPCR primers for each set) specific for miR-1224 is designed by Ribobio. DNAs were amplified by qPCR using SYBR Green reagent (Vazyme, Nanjing, China) on a 7900HT system (Applied Biosystems, USA). The primers used are listed in [Table S1](#).

#### Western blotting

Total protein was isolated from cells and tissues using radioimmuno-precipitation assay buffer containing protease and phosphatase inhib-

itor cocktails (Beyotime, Shanghai, China) in accordance with the manufacturer's protocols. Protein extracts were then separated by SDS-polyacrylamide gel electrophoresis and transferred to polyvinylidene fluoride (PVDF) membranes (Bio-Rad, Hercules, CA, USA) in transfer buffer. Then membranes were blocked with 5% non-fat dried milk for 2 h and incubated at 4°C with primary antibodies overnight. The next day, membranes were incubated at room temperature with the appropriate horseradish-peroxidase-conjugated secondary antibodies for 2 h and detected in an electro-chemiluminescence detection system (Thermo Fisher Scientific). The following primary antibodies were used: PCNA, cyclin D1, cyclin E1, P27, MST1/2, Lats1/2, p-Lats1, SAV1, YAP, H3K27me3, H3 (Cell Signaling Technology, Beverly, MA, USA), GAPDH, and lamin B (Proteintech, Wuhan, China).

#### Nude mouse model of xenograft

BALB/c-A nude mice (4 weeks old, n = 20) were purchased from the Animal Core Facility of Nanjing Medical University (Nanjing, China). Mice were randomly assigned into four groups (pretreated with lentivirus containing the pre-miRNA-1224, miRNA-1224 inhibitor, and respective NC sequences). Then,  $2 \times 10^6$  cells (suspended in 100 µL PBS) were subcutaneously injected into the respective flanks of each mouse. All mice were monitored every week and were sacrificed 5 weeks later. Tumor volume was measured with the following formula: volume = width<sup>2</sup> × 1/2length. All sections were stained with hematoxylin and eosin (H&E) and used for IHC. All animal studies were in accordance with the Institutional Animal Care and Use Committee of Nanjing Medical University.

#### IHC

All paraffin sections were dewaxed, rehydrated, and treated with 3% H<sub>2</sub>O<sub>2</sub> for 15 min to inhibit endogenous peroxidases and proteins. After heat-induced epitope retrieval in citrate buffer (10 mM, pH 6.0), the slides were incubated overnight at 4°C with prediluted primary antibodies raised against CREB, YAP, and Ki-67 (Cell Signaling Technology). After 1 h incubation with a secondary antibody at room temperature, the signal was developed with 3,3'-diaminobenzidine tetrachloride. The final score = score of staining intensity × score of staining percentage. Staining intensity was divided into 4 grades as follows: 0 (no staining), 1 (weak staining), 2 (intermediate staining), or 3 (strong staining). The staining percentage score depended on the rate of positive cells and was divided into the following grades: 0 for less than 5%, 1 for 5% to 25%, 2 for 25% to 50%, 3 for 50% to 75%, and 4 for greater than 75%.

#### Dual luciferase reporter assay

The WT and MUT 3' UTR segments of CREB-containing putative miR-1224 binding sites were cloned into the pGL3 plasmid (Ambion, Austin, TX, USA). HEK293T cells ( $5 \times 10^5$  cells per well) were then seeded into a 24-well plate and incubated for 24 h before being co-transfected with the WT or MUT reporter plasmid, a Renilla luciferase (pRL) plasmid (Promega, Madison, WI, USA), and the miR-1224 mimic or miR-NC. After transfection for 36 h, luciferase activities were then analyzed using the Dual Luciferase Reporter Assay System (Promega).

## FISH

The expression of miR-1224 was detected in HCC samples and normal liver tissues by FISH. The mature human miR-1224 sequence we used for detection was as follows: 5'-GGUGGAGGGCUCAGGA GUG-3'. The 5'-FAM-labeled miR-1224 probe sequence we used was 5'-CCACCTCCCGAGTCCTCAC-3' and was purchased from Ribobio. The FISH procedure followed the Ribobio instructions as described earlier.

## DNA methylation analysis

The methylation levels of the CpG islands located in the TSS of miR-1224 in Hep3B and HCCLM3 cell lines were assessed using BSP. The forward primer was 5'-GGATTYGGATTTAAAATGGT-3' and the reverse primer was 5'-AATCCTCACAAAAACAAATA-3'; these were used to amplify the genomic DNA sequences of CpG islands by PCR. The PCR products were separated by 3% agarose gel electrophoresis and then cloned into the pUC18 T-vector (Sangon, Shanghai, China). Following bacterial amplification of the cloned PCR fragments, 10 clones were conducted using DNA sequencing.

## ChIP assay

The ChIP assays were performed using Pierce magnetic ChIP kit (Thermo Fisher, Waltham, MA, USA) according to the manufacturer's instructions. In brief, HCCLM3 cells were cross-linked with formaldehyde and lysed. Then the lysate was immunoprecipitated with H3K27me3 antibody (Cell Signaling Technology) or with control immunoglobulin G (IgG; Cell Signaling Technology) at 4°C overnight. Reverse cross-linking and chromatin DNA purification followed the immunoprecipitations. ChIP DNA samples were analyzed by quantitative real-time PCR in an ABI7300 sequence detection system (Applied Biosystems), using specific primers listed in Table S2.

## Statistical analysis

All experimental data are presented as mean  $\pm$  SD from at least three independent experiments. Qualitative data were analyzed by the chi-square test. Differences between groups were analyzed by the Student's t test. The correlation between miR-1224 and CREB mRNA levels was analyzed by the Pearson's correlation test. OS and DFS were analyzed by the Kaplan-Meier method and the difference was assessed by log-rank test. All statistical analyses were performed by SPSS 24.0 (SPSS, Chicago, IL, USA) and Prism 7 (GraphPad Software, La Jolla, CA, USA). Statistical significance was considered when \* $p$  < 0.05, \*\* $p$  < 0.01, and \*\*\* $p$  < 0.001.

## ACKNOWLEDGMENTS

This study was supported by the Foundation of Jiangsu Collaborative Innovation Center of Biomedical Functional Materials, the Priority Academic Program Development of Jiangsu Higher Education Institutions, Jiangsu Graduate Research and Practice Innovation Program (SJCX20\_0474), The National Natural Science Foundation of China (81521004, 81871259, and 82070675), and Six Talent Peaks Project in Jiangsu Province (WSW-019).

## AUTHOR CONTRIBUTIONS

S.Y., C.Y., W.Y., and X.Y. performed the assays *in vitro*; G.S. and Y.H. performed the experiments *in vivo*; K.C. and F.C. collected clinical samples and analyzed the data; S.Y. and W.J. wrote the manuscript; L.L., J.R., F.Z., and X.W. designed this study. S.Y., W.J., and X.W. revised the paper. All authors have read and approved the final manuscript.

## DECLARATION OF INTERESTS

The authors declare no competing interests.

## REFERENCES

- Bray, F., Ferlay, J., Soerjomataram, I., Siegel, R.L., Torre, L.A., and Jemal, A. (2018). Global cancer statistics 2018: GLOBOCAN estimates of incidence and mortality worldwide for 36 cancers in 185 countries. *CA Cancer J. Clin.* 68, 394–424.
- Miller, K.D., Siegel, R.L., Lin, C.C., Mariotto, A.B., Kramer, J.L., Rowland, J.H., Stein, K.D., Alteri, R., and Jemal, A. (2016). Cancer treatment and survivorship statistics, 2016. *CA Cancer J. Clin.* 66, 271–289.
- Bosetti, C., Turati, F., and La Vecchia, C. (2014). Hepatocellular carcinoma epidemiology. *Best Pract. Res. Clin. Gastroenterol.* 28, 753–770.
- Bartel, D.P. (2009). MicroRNAs: target recognition and regulatory functions. *Cell* 136, 215–233.
- Shenouda, S.K., and Alahari, S.K. (2009). MicroRNA function in cancer: oncogene or a tumor suppressor? *Cancer Metastasis Rev.* 28, 369–378.
- Calin, G.A., Sevignani, C., Dumitru, C.D., Hyslop, T., Noch, E., Yendamuri, S., Shimizu, M., Rattan, S., Bullrich, F., Negrini, M., and Croce, C.M. (2004). Human microRNA genes are frequently located at fragile sites and genomic regions involved in cancers. *Proc. Natl. Acad. Sci. USA* 101, 2999–3004.
- Bartel, D.P. (2004). MicroRNAs: genomics, biogenesis, mechanism, and function. *Cell* 116, 281–297.
- Ha, M., and Kim, V.N. (2014). Regulation of microRNA biogenesis. *Nat. Rev. Mol. Cell Biol.* 15, 509–524.
- Wei, L., Wang, X., Lv, L., Liu, J., Xing, H., Song, Y., Xie, M., Lei, T., Zhang, N., and Yang, M. (2019). The emerging role of microRNAs and long noncoding RNAs in drug resistance of hepatocellular carcinoma. *Mol. Cancer* 18, 147.
- He, Y., Hwang, S., Cai, Y., Kim, S.J., Xu, M., Yang, D., Guillot, A., Feng, D., Seo, W., Hou, X., and Gao, B. (2019). MicroRNA-223 Ameliorates Nonalcoholic Steatohepatitis and Cancer by Targeting Multiple Inflammatory and Oncogenic Genes in Hepatocytes. *Hepatology* 70, 1150–1167.
- Mosakhani, N., Lahti, L., Borze, I., Karjalainen-Lindsberg, M.L., Sundström, J., Ristamäki, R., Osterlund, P., Knuutila, S., and Sarhadi, V.K. (2012). MicroRNA profiling predicts survival in anti-EGFR treated chemorefractory metastatic colorectal cancer patients with wild-type KRAS and BRAF. *Cancer Genet.* 205, 545–551.
- Nymark, P., Guled, M., Borze, I., Faisal, A., Lahti, L., Salmenkivi, K., Kettunen, E., Anttila, S., and Knuutila, S. (2011). Integrative analysis of microRNA, mRNA and aCGH data reveals asbestos- and histology-related changes in lung cancer. *Genes Chromosomes Cancer* 50, 585–597.
- Wang, J., Wen, T., Li, Z., Che, X., Gong, L., Yang, X., Zhang, J., Tang, H., He, L., Qu, X., and Liu, Y. (2019). MicroRNA-1224 Inhibits Tumor Metastasis in Intestinal-Type Gastric Cancer by Directly Targeting FAK. *Front. Oncol.* 9, 222.
- Li, L., Tang, J., Zhang, B., Yang, W., LiuGao, M., Wang, R., Tan, Y., Fan, J., Chang, Y., Fu, J., et al. (2015). Epigenetic modification of MiR-429 promotes liver tumour-initiating cell properties by targeting Rb binding protein 4. *Gut* 64, 156–167.
- Li, S., Chowdhury, R., Liu, F., Chou, A.P., Li, T., Mody, R.R., Lou, J.J., Chen, W., Reiss, J., Soto, H., et al. (2014). Tumor-suppressive miR148a is silenced by CpG island hypermethylation in IDH1-mutant gliomas. *Clin. Cancer Res* 20, 5808–5822.
- Lee, K.P., Lee, J.H., Kim, T.S., Kim, T.H., Park, H.D., Byun, J.S., Kim, M.C., Jeong, W.I., Calvisi, D.F., Kim, J.M., and Lim, D.S. (2010). The Hippo-Salvador pathway restrains hepatic oval cell proliferation, liver size, and liver tumorigenesis. *Proc. Natl. Acad. Sci. USA* 107, 8248–8253.

17. Kim, W., Khan, S.K., Liu, Y., Xu, R., Park, O., He, Y., Cha, B., Gao, B., and Yang, Y. (2018). Hepatic Hippo signaling inhibits protumoural microenvironment to suppress hepatocellular carcinoma. *Gut* 67, 1692–1703.
18. Lu, H., Kojima, K., Battula, V.L., Korchin, B., Shi, Y., Chen, Y., Spong, S., Thomas, D.A., Kantarjian, H., Lock, R.B., et al. (2014). Targeting connective tissue growth factor (CTGF) in acute lymphoblastic leukemia preclinical models: anti-CTGF monoclonal antibody attenuates leukemia growth. *Ann. Hematol.* 93, 485–492.
19. Garcia, P., Leal, P., Ili, C., Brebi, P., Alvarez, H., and Roa, J.C. (2013). Inhibition of connective tissue growth factor (CTGF/CCN2) in gallbladder cancer cells leads to decreased growth in vitro. *Int. J. Exp. Pathol.* 94, 195–202.
20. Zhang, Y., Yang, J., Cui, X., Chen, Y., Zhu, V.F., Hagan, J.P., Wang, H., Yu, X., Hodges, S.E., Fang, J., et al. (2013). A novel epigenetic CREB-miR-373 axis mediates ZIP4-induced pancreatic cancer growth. *EMBO Mol. Med.* 5, 1322–1334.
21. Chen, Z., Li, J.L., Lin, S., Cao, C., Gimbrone, N.T., Yang, R., Fu, D.A., Carper, M.B., Haura, E.B., Schabath, M.B., et al. (2016). cAMP/CREB-regulated LINC00473 marks LKB1-inactivated lung cancer and mediates tumor growth. *J. Clin. Invest.* 126, 2267–2279.
22. Zhang, T., Zhang, J., You, X., Liu, Q., Du, Y., Gao, Y., Shan, C., Kong, G., Wang, Y., Yang, X., et al. (2012). Hepatitis B virus X protein modulates oncogene Yes-associated protein by CREB to promote growth of hepatoma cells. *Hepatology* 56, 2051–2059.
23. Liu, Y., Li, X., Zhang, Y., Wang, H., Rong, X., Peng, J., He, L., and Peng, Y. (2019). An miR-340-5p-macrophage feedback loop modulates the progression and tumor microenvironment of glioblastoma multiforme. *Oncogene* 38, 7399–7415.
24. Wang, Y., Wu, M., Lei, Z., Huang, M., Li, Z., Wang, L., Cao, Q., Han, D., Chang, Y., Chen, Y., et al. (2018). Dysregulation of miR-6868-5p/FOXO1 circuit contributes to colorectal cancer angiogenesis. *J. Exp. Clin. Cancer Res.* 37, 292.
25. Esteller, M. (2007). Cancer epigenomics: DNA methylomes and histone-modification maps. *Nat. Rev. Genet.* 8, 286–298.
26. Taby, R., and Issa, J.P. (2010). Cancer epigenetics. *CA Cancer J. Clin.* 60, 376–392.
27. Zhang, Y., Zheng, D., Zhou, T., Song, H., Hulsurkar, M., Su, N., Liu, Y., Wang, Z., Shao, L., Ittmann, M., et al. (2018). Androgen deprivation promotes neuroendocrine differentiation and angiogenesis through CREB-EZH2-TSP1 pathway in prostate cancers. *Nat. Commun.* 9, 4080.
28. Hanahan, D., and Weinberg, R.A. (2011). Hallmarks of cancer: the next generation. *Cell* 144, 646–674.
29. Della Vittoria Scarpati, G., Falcetta, F., Carlomagno, C., Ubezio, P., Marchini, S., De Stefano, A., Singh, V.K., D'Incalci, M., De Placido, S., and Pepe, S. (2012). A specific miRNA signature correlates with complete pathological response to neoadjuvant chemoradiotherapy in locally advanced rectal cancer. *Int. J. Radiat. Oncol. Biol. Phys.* 83, 1113–1119.
30. Hu, C., Cheng, X., MingYu, Q., Wang, X.B., and Shen, S.Q. (2019). The effects of microRNA-1224-5p on hepatocellular carcinoma tumor endothelial cells. *J. Cancer Res. Ther.* 15, 329–335.
31. Lu, L., Li, Y., Kim, S.M., Bossuyt, W., Liu, P., Qiu, Q., Wang, Y., Halder, G., Finegold, M.J., Lee, J.S., and Johnson, R.L. (2010). Hippo signaling is a potent in vivo growth and tumor suppressor pathway in the mammalian liver. *Proc. Natl. Acad. Sci. USA* 107, 1437–1442.
32. Yimlamai, D., Fowl, B.H., and Camargo, F.D. (2015). Emerging evidence on the role of the Hippo/YAP pathway in liver physiology and cancer. *J. Hepatol.* 63, 1491–1501.
33. Pan, D. (2007). Hippo signaling in organ size control. *Genes Dev.* 21, 886–897.
34. Halder, G., and Johnson, R.L. (2011). Hippo signaling: growth control and beyond. *Development* 138, 9–22.
35. Piccolo, S., Dupont, S., and Cordenonsi, M. (2014). The biology of YAP/TAZ: hippo signaling and beyond. *Physiol. Rev.* 94, 1287–1312.
36. Oh, H., and Irvine, K.D. (2008). In vivo regulation of Yorkie phosphorylation and localization. *Development* 135, 1081–1088.
37. Vassilev, A., Kaneko, K.J., Shu, H., Zhao, Y., and DePamphilis, M.L. (2001). TEAD/TEF transcription factors utilize the activation domain of YAP65, a Src/Yes-associated protein localized in the cytoplasm. *Genes Dev.* 15, 1229–1241.
38. Lai, D., Ho, K.C., Hao, Y., and Yang, X. (2011). Taxol resistance in breast cancer cells is mediated by the hippo pathway component TAZ and its downstream transcriptional targets Cyr61 and CTGF. *Cancer Res.* 71, 2728–2738.
39. Hsu, Y.L., Hung, J.Y., Chou, S.H., Huang, M.S., Tsai, M.J., Lin, Y.S., Chiang, S.Y., Ho, Y.W., Wu, C.Y., and Kuo, P.L. (2015). Angiotensin decreases lung cancer progression by sequestering oncogenic YAP/TAZ and decreasing Cyr61 expression. *Oncogene* 34, 4056–4068.
40. Ni, X., Tao, J., Barbi, J., Chen, Q., Park, B.V., Li, Z., Zhang, N., Lebid, A., Ramaswamy, A., Wei, P., et al. (2018). YAP Is Essential for Treg-Mediated Suppression of Antitumor Immunity. *Cancer Discov.* 8, 1026–1043.
41. Qian, J., Li, R., Wang, Y.Y., Shi, Y., Luan, W.K., Tao, T., Zhang, J.X., Xu, Y.C., and You, Y.P. (2015). MiR-1224-5p acts as a tumor suppressor by targeting CREB1 in malignant gliomas. *Mol. Cell. Biochem.* 403, 33–41.
42. Sakamoto, K.M., and Frank, D.A. (2009). CREB in the pathophysiology of cancer: implications for targeting transcription factors for cancer therapy. *Clin. Cancer Res.* 15, 2583–2587.
43. Thway, K., and Fisher, C. (2012). Tumors with EWSR1-CREB1 and EWSR1-ATF1 fusions: the current status. *Am. J. Surg. Pathol.* 36, e1–e11.
44. Tang, Y., Berling, J., and Mavila, N. (2018). Inhibition of CREB binding protein-beta-catenin signaling down regulates CD133 expression and activates PP2A-PTEN signaling in tumor initiating liver cancer cells. *Cell Commun. Signal.* 16, 9.
45. Yu, L., Guo, X., Zhang, P., Qi, R., Li, Z., and Zhang, S. (2014). Cyclic adenosine monophosphate-responsive element-binding protein activation predicts an unfavorable prognosis in patients with hepatocellular carcinoma. *OncoTargets Ther.* 7, 873–879.
46. Wang, J., Ma, L., Weng, W., Qiao, Y., Zhang, Y., He, J., Wang, H., Xiao, W., Li, L., Chu, Q., et al. (2013). Mutual interaction between YAP and CREB promotes tumorigenesis in liver cancer. *Hepatology* 58, 1011–1020.
47. Varshney, A., Panda, J.J., Singh, A.K., Yadav, N., Bihari, C., Biswas, S., Sarin, S.K., and Chauhan, V.S. (2018). Targeted delivery of microRNA-199a-3p using self-assembled dipeptide nanoparticles efficiently reduces hepatocellular carcinoma in mice. *Hepatology* 67, 1392–1407.
48. Revia, R.A., Stephen, Z.R., and Zhang, M. (2019). Theranostic Nanoparticles for RNA-Based Cancer Treatment. *Acc. Chem. Res.* 52, 1496–1506.
49. Landmesser, U., Poller, W., Tsimikas, S., Most, P., Paneni, F., and Lüscher, T.F. (2020). From traditional pharmacological towards nucleic acid-based therapies for cardiovascular diseases. *Eur. Heart J.* 41, 3884–3899.
50. Zuo, X., Chen, Z., Gao, W., Zhang, Y., Wang, J., Wang, J., Cao, M., Cai, J., Wu, J., and Wang, X. (2020). M6A-mediated upregulation of LINC00958 increases lipogenesis and acts as a nanotherapeutic target in hepatocellular carcinoma. *J. Hematol. Oncol.* 13, 5.
51. Vondran, F.W., Katenz, E., Schwartlander, R., Morgul, M.H., Raschzok, N., Gong, X., Cheng, X., Kehr, D., and Sauer, I.M. (2008). Isolation of primary human hepatocytes after partial hepatectomy: criteria for identification of the most promising liver specimen. *Artif. Organs* 32, 205–213.